JACS
JOURNAL OF THE AMERICAN CHEMICAL SOCIETY
Communication
pubs.acs.org/JACS

Spinel Mn−Co Oxide in N-Doped Carbon Nanotubes as a Bifunctional Electrocatalyst Synthesized by Oxidative Cutting

Anqi Zhao,[†] Justus Masa,[‡] Wei Xia,[†] Artjom Maljusch,[‡] Marc-Georg Willinger,[§] Guylhaine Clavel,[§] Kunpeng Xie,[†] Robert Schlögl,[§] Wolfgang Schuhmann,*[,‡] and Martin Muhler*[,†]

[†]Laboratory of Industrial Chemistry, Ruhr-University Bochum, 44801 Bochum, Germany
[‡]Analytical Chemistry - Center for Electrochemical Sciences (CES), Ruhr-University Bochum, D-44780 Bochum, Germany
[§]Fritz-Haber Institute of the Max-Planck Society, 14195 Berlin, Germany

Supporting Information

ABSTRACT: The notorious instability of non-precious-metal catalysts for oxygen reduction and evolution is by far the single unresolved impediment for their practical applications. We have designed highly stable and active bifunctional catalysts for reversible oxygen electrodes by oxidative thermal scission, where we concurrently rupture nitrogen-doped carbon nanotubes and oxidize Co and Mn nanoparticles buried inside them to form spinel Mn−Co oxide nanoparticles partially embedded in the nanotubes. Impressively high dual activity for oxygen reduction and evolution is achieved using these catalysts, surpassing those of Pt/C, RuO_2, and IrO_2 and thus raising the prospect of functional low-cost, non-precious-metal bifunctional catalysts in metal−air batteries and reversible fuel cells, among others, for a sustainable and green energy future.

Decentralized supply of energy from renewable sources strongly relies on the efficient conversion and storage of energy in different forms, for example, in the form of H_2 by electrolysis of water and recovery of the energy during the reverse process in fuel cells[1] and in rechargeable metal−air batteries.[2] Whereas the reversibility of the electrochemical reactions involving H_2 in the case of regenerative fuel cells and reduced metal in the case of metal−air batteries is efficient, the main challenge lies in improving the efficiency of the oxygen reduction reaction (ORR) and the oxygen evolution reaction (OER). Platinum, the state-of-the-art electrocatalyst for the ORR, is poor for the OER, while Ru and Ir oxides, the best known electrocatalysts for the OER, are poor for the ORR.[3−5] Several strategies have been suggested to overcome this conundrum, which include, among others, the design of multicomponent bifunctional catalysts capable of driving both reactions by combining good catalysts for ORR with those for OER into a composite.

Recently, transition-metal-based catalysts such as Mn and Co oxides have attracted enormous interest as low-cost alternatives to noble-metal catalysts capable of catalyzing both the ORR and the OER.[5,6] However, these oxides have high electrical resistance, which fortunately can be mitigated by the use of conductive additives such as graphene[7] and carbon nanotubes (CNTs).[8] In particular, N-doped carbon materials have been widely used not only to promote electron transfer but also to serve as complementary sites for the ORR, thereby enhancing the ability of the materials to electrocatalyze both the ORR and the OER.[2,9] Dai and co-workers reported that cobalt oxide supported on N-doped graphene[6] and spinel manganese−cobalt oxide supported on N-doped reduced graphene oxide[10] exhibited high ORR and OER activities. The high catalytic activity of supported oxide nanoparticles is thought to be facilitated by the strong coupling between oxide nanoparticles and the support, which however cannot be easily achieved, for example, by impregnation or precipitation methods. Insufficient contact between metal oxides and carbon often leads to high contact resistance and thus low electron transfer efficiency, resulting in poor electrocatalytic performance.

Here we report a simple, scalable, and novel method for the synthesis of spinel Mn−Co oxide nanoparticles partially embedded in N-doped CNTs (NCNTs) by oxidative thermal scission, where we concurrently rupture NCNTs and oxidize the residual catalyst particles (Mn and Co) buried in them. Because of the intimate contact between the metal oxide and the graphene walls, the obtained samples showed excellent performance as bifunctional electrocatalysts for both the ORR and OER under alkaline conditions.

The synthesis of the spinel Mn−Co oxide catalysts partially embedded in NCNTs is schematically shown in Figure 1. NCNTs with outer diameters of 13−16 nm synthesized by catalytic growth using Co−Mn−Mg−Al mixed oxide catalysts and pyridine as the carbon- and nitrogen-containing precursor were used as the starting material.[11] Studies showed that the catalyst nanoparticles exist in two different forms, either (a) at the tip of the NCNTs or enclosed inside the NCNTs, where the nanoparticles are intimately in contact with carbon, or (b) scattered over the NCNT agglomerates without intimate contact with the carbon surface[11,12] as a result of explosion-like fragmentation of the initial catalyst particles during the rapid growth.[13] Long-time washing of the NCNTs with dilute HNO_3 at room temperature removed the exposed metal species that were not in intimate contact with carbon. Subsequently, the washed NCNTs still containing the encapsulated catalyst nanoparticles were thermally treated under flowing air by moving the reactor into a heated furnace and withdrawing it from the heating zone after 5 min (Figure 1). This process

Received: March 12, 2014
Published: May 9, 2014

   dx.doi.org/10.1021/ja502532y | J. Am. Chem. Soc. 2014, 136, 7551−7554

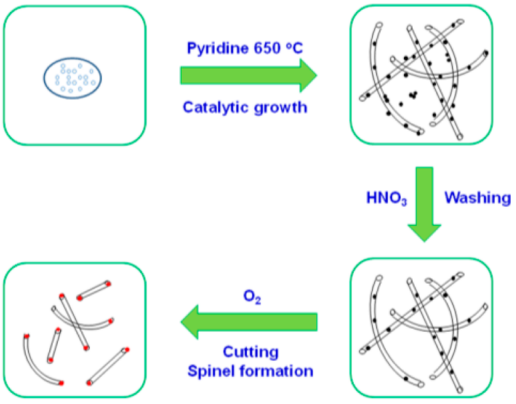

Figure 1. Synthesis of spinel Mn−Co oxide nanoparticles partially embedded in NCNTs. (1) catalytic growth of NCNTs using a Co−Mn−Al−Mg catalyst. (2) Removal of exposed catalyst nanoparticles with poor contact with carbon by washing in dilute HNO_3. (3) Formation of spinel oxide partially embedded in NCNTs by short exposure to air at elevated temperatures (oxidative cutting).

causes opening and rupture of the CNTs through oxidation and thermal stress.[14] Different temperatures from 300 to 600 °C were applied, and the heating process was repeated three times at each temperature. The obtained samples are designated as NCNT-300, NCNT-400, NCNT-500, and NCNT-600.

Thermogravimetry (Figure S2 in the Supporting Information) and temperature-programmed oxidation[15] studies revealed that oxidation of the NCNTs begins at about 300 °C. Depending on the applied temperature, the thermal treatment leads to oxidation of carbon preferentially around the catalyst nanoparticles[16] and simultaneous oxidation of the encapsulated catalysts, in this case metallic Co in close contact with Mn oxides. The contents of Mn and Co in the washed NCNTs were determined by inductively coupled plasma optical emission spectroscopy (ICP-OES) and found to be 0.59 and 1.12 wt %, respectively (Table S1 in the Supporting Information).

The weight loss of NCNTs increased with increasing oxidation temperature (Table S2), while the percentage weight of Mn and Co increased as a result of the loss of carbon through oxidation (Table S1). It is worth noting that despite these changes, the Mn/Co molar ratio remained at about 1:2 in all of the samples. Moderate oxidation led to an increase in specific surface area (Table S3), and Raman spectroscopy revealed an increase in surface defects (Figure S3).

Only carbon reflections were observed at 26.03° (002) and 43.46° (100)/(101) in the X-ray diffraction (XRD) pattern of the washed NCNTs (Figure 2a), whereas metal species were not detected. The carbon reflections of the NCNTs are slightly shifted to smaller 2θ due to lattice distortion caused by the incorporated nitrogen atoms.[17] The oxidative treatment at 300 °C did not cause significant changes to NCNT. After treatment at 400 °C, diffraction peaks of spinel Mn−Co oxide became discernible, and their intensity increased with increasing treatment temperature, indicating sintering of the oxide nanoparticles. On the other hand, the relative intensity of the carbon reflections diminished with increasing temperature, indicating a decrease in structural order or the formation of defects.

The formation of Mn−Co oxide nanoparticles was confirmed by high-resolution transmission electron microscopy (HRTEM) studies (Figure 2b−d). Both Mn and Co as well

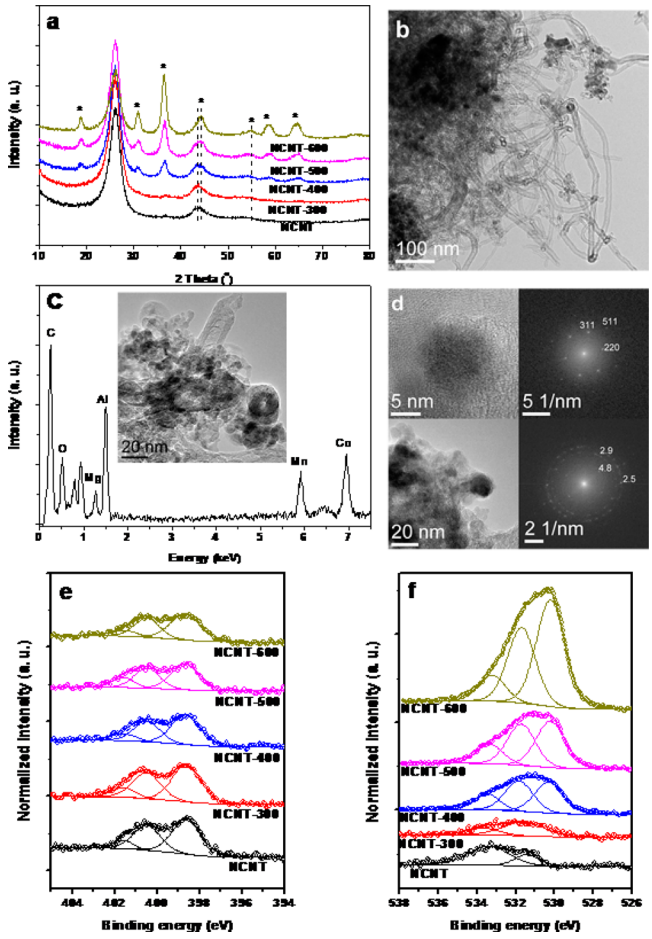

Figure 2. (a) XRD patterns. Spinel Mn−Co oxide peaks are identified by *. (b) TEM image showing an overview of NCNT-500. (c) EDX spectrum from a region containing tubes and particles of NCNT-500. (d) HRTEM images with corresponding power spectra of an isolated particle and a bunch of particles of NCNT-400. (e) N 1s and (f) O 1s XP spectra.

as Al and Mg were detected by EDX in the sample (Figure 2c). The lattice spacings observed for different particles (Figure 2d) are consistent with a cubic spinel structure, in agreement with the XRD results. Additionally, the Mn/Co ratio of 1:2 further confirms the presence of spinel Mn−Co oxide ($MnCo_2O_4$).

The surface chemistry of the samples was studied by X-ray photoelectron spectroscopy (XPS). Only C, N, and O were detected in the washed NCNTs and NCNT-300. Mn and Co species were detected after oxidative cutting at temperatures above 400 °C. The cutting did not cause significant changes in the C 1s and N 1s spectra even at high temperatures (Figure 2e), whereas the oxygen peak increased significantly, as indicated by the stronger O 1s peaks at 530.2 eV (Figure 2f), confirming the formation of metal oxides. Interestingly, the increase in surface oxygen bound to carbon was insignificant, which is important for electrocatalysis, since too much surface oxygen can considerably increase the electrical resistance of carbon materials as well as the hydrophilicity of the exposed carbon surface. High resistance impedes electron transfer during catalysis, while strong hydrophilicity hinders the release of water during the ORR, leading to flooding of the electrode. It is important to note that the composition of nitrogen was not significantly affected by the oxidative treatment even at 600 °C (Figure 2e). Therefore, nitrogen was conserved while spinel

dx.doi.org/10.1021/ja502532y | J. Am. Chem. Soc. 2014, 136, 7551−7554

Mn−Co oxide was formed, and the favorable surface properties of NCNTs were not significantly affected by the oxidative treatment.

The electrocatalytic activity was evaluated in 0.1 M KOH with a catalyst loading of 210 μg cm^{-2} (see the Supporting Information for details). Redox features reminiscent of transitions from metallic species were clearly discernible in the voltammograms of NCNT-400 recorded under argon, whereas they were indiscernible for NCNT-300 (Figure S5), in good agreement with the XRD results.

Thermal oxidative cutting of the NCNTs drastically enhanced the ORR activity of the catalysts, as indicated by the linear sweep voltammograms in Figure 3a. NCNT-300

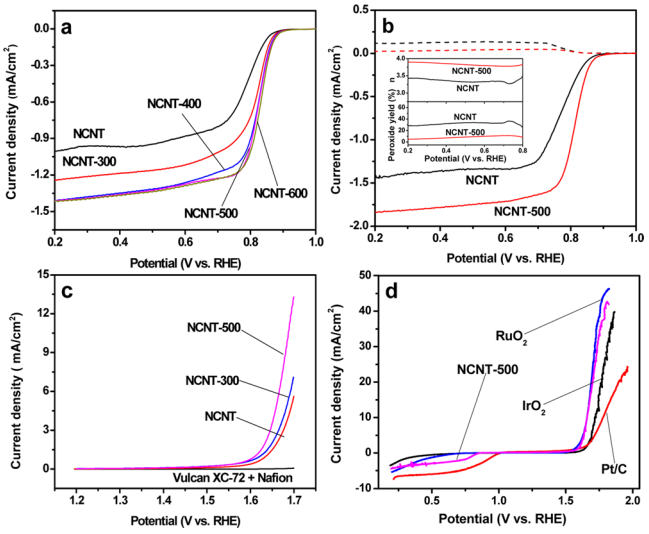

Figure 3. (a) Linear sweep voltammograms at 100 rpm and 5 mV s^{-1}. (b) RRDE voltammograms at 400 rpm and 5 mV s^{-1}. Inset: peroxide yield and electron transfer number (n) at various potentials. (c) OER current densities of the blank experiment (glassy carbon modified with vulcan XC-72/nafion), NCNTs, NCNT-300, and NCNT-500 at 1 mV s^{-1}. The recorded data were *IR*-corrected using the solution resistance as measured by electrochemical impedance spectroscopy at the open-circuit potential. (d) ORR and OER activities of NCNT-500, Pt/C, IrO_2, and RuO_2 at a scan rate of 5 mV s^{-1}. All of the voltammograms were recorded in O_2-saturated 0.1 M KOH.

exhibited a more positive onset potential and a higher reduction current than the washed nonoxidized NCNTs, suggesting a higher catalytic activity for the ORR. Further improvement in the ORR activity was observed for NCNT-400, while only a slight enhancement of the activity was observed when the temperature was increased from 400 to 600 °C. Besides the nitrogen-modified carbon species, which are well-known to catalyze the ORR, the spinel Mn−Co oxides formed by oxidative cutting are also expected to contribute active sites for the ORR.[6,7] To confirm the role of the spinel oxides, the samples obtained by the thermal oxidative cutting were washed in dilute nitric acid at room temperature and under stirring for 72 h to remove the metal oxide nanoparticles. The acid-washed samples showed much lower activities, as indicated by the shift in the onset potential to lower values (Figure S6). Hence, the spinel Mn−Co oxide formed during oxidative cutting plays an essential role in ORR catalysis.

The catalytic pathways for the ORR on NCNTs and NCNT-500 were investigated by rotating ring−disk electrode (RRDE) voltammetry (Figure 3b). Evidently, NCNT-500 exhibited superior catalytic performance compared with NCNTs, as indicated by a more positive onset potential and higher disk current for the ORR. Moreover, NCNT-500 had a lower ring current, indicating less production of H_2O_2 relative to NCNTs. The H_2O_2 yields and electron transfer numbers (n) for NCNTs and NCNT-500 at various potentials are shown in the inset of Figure 3b. The yield of H_2O_2 was approximately 5% at 0.2 V for NCNT-500, which is significantly lower than the yield of 29% for NCNTs. The average electron transfer numbers were 3.8 and 3.4 for NCNT-500 and NCNTs, respectively, over the potential range from 0.8 to 0.2 V, suggesting the prevalence of both the four-electron and two-electron ORR reduction pathways in both cases. However, on the basis of the amount of H_2O_2 produced, it is very clear that the ORR on NCNTs produces more HO_2^-, which is then further reduced to OH^- or goes through a cycle of disproportionation and oxygen reduction, ultimately converting all of the oxygen to OH^-. For NCNT-500, the reaction was dominated by the four-electron pathway, confirming a higher selectivity of the ORR to OH^- on NCNT-500. This result shows that the Mn−Co oxide active sites complement those of the NCNTs, leading to the significantly improved ORR activity of NCNT-500. Interestingly, the selectivity of NCNT-500 concurs very well with the results reported by Liang et al.[10] for a covalent hybrid of spinel manganese−cobalt oxide and N-doped graphene

The ability of the obtained catalysts to catalyze both the ORR and the OER, that is, to serve as bifunctional catalysts, was investigated by rotating disk electrode (RDE) voltammetry and compared with those of state-of-art catalysts: Pt/C (20% Pt on Vulcan carbon), RuO_2, and IrO_2. Studies of the OER (Figure 3c) revealed that NCNT-500 had the best activity. Remarkably, NCNT-500 showed a higher ORR activity than IrO_2 and RuO_2 and an OER activity very similar to that of RuO_2 (Figure 3d). The onset potential of the OER was determined using scanning electrochemical microscopy (SECM) by in situ detection of evolved oxygen (Figures S1 and S7). An increase in the cathodic current measured at the tip commenced at about 1.495 V vs RHE, representing overpotential of only 0.265 V from the theoretical value of 1.23 V. The onset potential for the OER on non-oxidized NCNTs was observed at 1.515 V vs RHE. Durability measurements of NCNT-500 as a bifunctional catalyst showed a degradation tendency similar to that of RuO_2 over the same time scale (Figure S8), which suggests that this catalyst has durability comparable to that of RuO_2. These results therefore underscore the huge potential of thermal oxidative cutting for the synthesis of excellent bifunctional catalysts for oxygen electrodes.

In conclusion, a simple, easily scalable, and novel method for the synthesis of spinel Mn−Co oxide nanoparticles partially embedded in nitrogen-doped carbon nanotubes has been developed. Thermal oxidative treatment of catalytically grown NCNTs in which residual Co and Mn oxide nanoparticles are buried simultaneously ruptures the NCNTs and oxidizes the Co and Mn oxide nanoparticles, forming spinel Mn−Co oxide nanoparticles partially embedded in the NCNTs. The nitrogen-functionalized carbon groups in NCNTs, which act as active sites for oxygen reduction, are conserved during the thermal oxidative treatment process. As a result of a synergetic effect from the nitrogen groups in the NCNTs and the spinel Mn−Co oxide particles, the capability of the resulting catalysts to electrolyze both the ORR and the OER becomes tremendously enhanced, producing exceptionally active bifunctional catalysts for reversible oxygen electrodes.

dx.doi.org/10.1021/ja502532y | *J. Am. Chem. Soc.* 2014, 136, 7551−7554

■ ASSOCIATED CONTENT

Supporting Information

Experimental details and ICP-OES, TG, physisorption, Raman, CV, SECM, and stability data. This material is available free of charge via the Internet at http://pubs.acs.org.

■ AUTHOR INFORMATION

Corresponding Authors

muhler@techem.rub.de
wolfgang.schuhmann@rub.de

Notes

The authors declare no competing financial interest.

■ ACKNOWLEDGMENTS

Financial support from the Cluster of Excellence RESOLV (EXC 1069) funded by the Deutsche Forschungsgemeinschaft is gratefully acknowledged. A.Z. thanks the China Scholarship Council for a Ph.D. fellowship.

■ REFERENCES

(1) Chen, G.; Bare, S. R.; Mallouk, T. E. *J. Electrochem. Soc.* **2002**, *149*, A1092.
(2) Chen, Z.; Yu, A.; Ahmed, R.; Wang, H.; Li, H.; Chen, Z. *Electrochim. Acta* **2012**, *69*, 295.
(3) Chen, Z.; Waje, M.; Li, W.; Yan, Y. *Angew. Chem.* **2007**, *119*, 4138.
(4) Trasatti, S. *Electrochim. Acta* **1984**, *29*, 1503.
(5) Gorlin, Y.; Jaramillo, T. F. *J. Am. Chem. Soc.* **2010**, *132*, 13612.
(6) Liang, Y.; Li, Y.; Wang, H.; Zhou, J.; Wang, J.; Regier, T.; Dai, H. *Nat. Mater.* **2011**, *10*, 780.
(7) Feng, J.; Liang, Y.; Wang, H.; Li, Y.; Zhang, B.; Zhou, J.; Wang, J.; Regier, T.; Dai, H. *Nano Res.* **2012**, *5*, 718.
(8) Yang, Z.; Zhou, X.; Nie, H.; Yao, Z.; Huang, S. *ACS Appl. Mater. Interfaces* **2011**, *3*, 2601.
(9) Liang, Y.; Wang, H.; Diao, P.; Chang, W.; Hong, G.; Li, Y.; Gong, M.; Xie, L.; Zhou, J.; Wang, J.; Regier, T. Z.; Wei, F.; Dai, H. *J. Am. Chem. Soc.* **2012**, *134*, 15849.
(10) Liang, Y.; Wang, H.; Zhou, J.; Li, Y.; Wang, J.; Regier, T.; Dai, H. *J. Am. Chem. Soc.* **2012**, *134*, 3517.
(11) Tessonnier, J.-P.; Becker, M.; Xia, W.; Girgsdies, F.; Blume, R.; Yao, L.; Su, D. S.; Muhler, M.; Schlögl, R. *ChemCatChem* **2010**, *2*, 1559.
(12) Becker, M. J.; Xia, W.; Tessonnier, J.-P.; Blume, R.; Yao, L.; Schlögl, R.; Muhler, M. *Carbon* **2011**, *49*, 5253.
(13) Voelskow, K.; Nickelsen, L.; Becker, M. J.; Xia, W.; Muhler, M.; Kunz, U.; Weber, A. P.; Turek, T. *Chem. Eng. J.* **2013**, *234*, 74.
(14) Tran, M. Q.; Tridech, C.; Alfrey, A.; Bismarck, A.; Shaffer, M. S. P. *Carbon* **2007**, *45*, 2341.
(15) Zhao, A.; Masa, J.; Schuhmann, W.; Xia, W. *J. Phys. Chem. C* **2013**, *117*, 24283.
(16) Jin, C.; Xia, W.; Chen, P.; Muhler, M. *Catal. Today* **2012**, *186*, 128.
(17) Qu, L.; Liu, Y.; Baek, J.-B.; Dai, L. *ACS Nano* **2010**, *4*, 1321.